J. Electroanal. Chem., 270 (1989) 205–224
Elsevier Sequoia S.A., Lausanne – Printed in The Netherlands

Kinetics and mechanism of "reduced CO_2" electrooxidation on electrodispersed platinum in different acid solutions

M.L. Marcos, J. González-Velasco and J.M. Vara

Departamento de Electroquímica, Facultad de Ciencias, Universidad Autónoma de Madrid, Canto Blanco, (28049) Madrid (Spain)

M.C. Giordano and A.J. Arvia *

Instituto de Investigaciones Fisicoquímicas Teóricas y Aplicadas (INIFTA), Facultad de Ciencias Exactas, Universidad Nacional de La Plata, Sucursal 4, Casilla de Correo 16, (1900) La Plata (Argentina)

(Received 18 May 1988; in revised form 24 April 1989)

ABSTRACT

The electrooxidation of "reduced CO_2" electroadsorbates on electrodispersed platinum electrodes has been investigated in 0.05 *M* $HClO_4$, 1 *M* $HClO_4$, 0.5 *M* H_2SO_4 and 1 *M* H_3PO_4 at 25 °C through voltammetry and potential step techniques. The overall reaction comprises three distinguishable processes, namely a first order triggering process, and two second order surface processes. The latter are influenced remarkably by the solution composition (anions). The second order reaction mechanism involves two distinguishable "reduced CO_2" electroadsorbates which react independently with the OH species formed from H_2O electrooxidation on the bare platinum sites as the reaction proceeds. An interaction term has to be included in the rate equations to account for the experimental results. The mechanistic interpretation accounts for the values of the number of electrons per site ranging from 1 to 2.

INTRODUCTION

The electrochemical behaviour of "reduced" CO_2 has been the subject of many investigations from the standpoint of both the behaviour of organic residues at electrodes and the generation of an adsorbate which is attractive for electrosynthetic purposes [1–8]. Recent work on the subject [9,10] showed that the transient response of the reaction on bright Pt depends considerably on the composition of the electrolyte and the electrode surface pretreatment. These dependences were interpreted through a relatively simple reaction mechanism particularly sensitive to changes

* To whom correspondence should be addressed.

0022-0728/89/$03.50

in the value of the adsorption interaction parameter as defined through a Temkin-type isotherm.

The possibility of preparing electrodispersed platinum electrode surfaces [11] with reproducible and defined topography and roughness, offers an opportunity to reinvestigate the kinetics of the electrooxidation of CO_2 electroadsorbates under better defined electrocatalyst surface conditions [12]. Furthermore, the use of a large surface area electrode diminishes considerably the possible influence of impurities in the solution on the kinetics of the reaction. The voltammetric characteristics of electrodispersed Pt electrodes as far as this reaction is concerned [13], show that at relatively low sweep rates and surface roughness factors ranging from 5 to approximately 200, the entire surface is active and the kinetics of the reaction are free of the ohmic-type polarization usually found for porous-type platinized platinum electrodes.

The present work is devoted to investigating the kinetics of reduced CO_2 electrooxidation by using conventional voltammetric and current transient data with the purpose of distinguishing amongst different possible reactions contributing to the overall process and evaluating the corresponding rate constants. The kinetic interpretation accounts for the initiation of the electrooxidation process from the electrode surface with the electroadsorbate at maximum coverage.

EXPERIMENTAL

The experimental work comprised the preparation of the electrodispersed platinum electrodes starting from bright platinum wires (0.05 cm dia), the electroformation of the CO_2 electroadsorbate and its subsequent electrooxidation, either voltammetrically or potentiostatically.

The working electrodes were prepared by the electrochemical technique already described in a previous publication [11], which in short consists of first accumulating a platinum oxide layer by applying a fast periodic perturbing potential to the electrode in acid solution, and subsequently electroreducing the oxide layer by means of a slow potential scan. The resulting topography of the electrodispersed platinum surface has been well characterized through SEM and STM imaging [11,12]. The corresponding roughness factor can be defined as the ratio between either the H-adatom or the O-adatom voltammetric charge of the electrodispersed platinum and that of the original smooth surface platinum.

Previous studies made in 1 M $HClO_4$ and 0.5 M H_2SO_4 [13] were extended to 0.05 M $HClO_4$ and 1 M H_3PO_4. Solutions were prepared with triply distilled water. Runs were made at 25° C.

Voltammetric results were obtained by applying the potential–time programme shown in Fig. 1 (see inset potential programme). The potential sweep rate (v) was changed from 0.005 V/s to 0.4 V/s.

Potentiostatic transients were recorded by employing different adsorption potentials (E_{ad}) at either both constant adsorption time (t_{ad}) and oxidation potential (E_{ox}), or by keeping E_{ox} constant and changing t_{ad}. Recordings were also obtained

by keeping E_{ad} and t_{ad} constant and changing E_{ox}, to cover systematically the various possible combinations. As had been established previously [13], for a roughness factor, R, between 5 and 200, the behaviour of electrodispersed platinum electrodes is independent of R, at least for $v < 0.05$ V/s. In the present work most runs were made with electrodispersed platinum electrodes with $R = 21$ and $R = 70$. In this case the values of R denote the O-adatom voltammetric electrodesorption charge ratio determined at 0.2 V/s before and after the RSWPS treatment as described in previous publications [11,13]. Potentials in the text are referred to the reversible saturated hydrogen electrode (SHE) in the same solution.

RESULTS

Voltammetric data

The voltammetric electrooxidation of electroadsorbed CO_2 at electrodispersed platinum depends strongly on the electrolyte composition (Fig. 1a). The electrochemical reaction gives a complex, rather symmetric anodic peak at ca. 0.64 V in 0.5 M H_2SO_4, at 0.63 V followed by a small shoulder at ca. 0.67 V in 1 M $HClO_4$, and two clear anodic current contributions, namely a peak at 0.64 V and a shoulder at ca. 0.72 V, in 1 M H_3PO_4. The latter becomes a well-defined current peak as v increases (Fig. 1b).

The pseudocapacitance–potential plots for the three acids exhibit clear maxima which are located more positively as v increases (Fig. 2). The existence of two

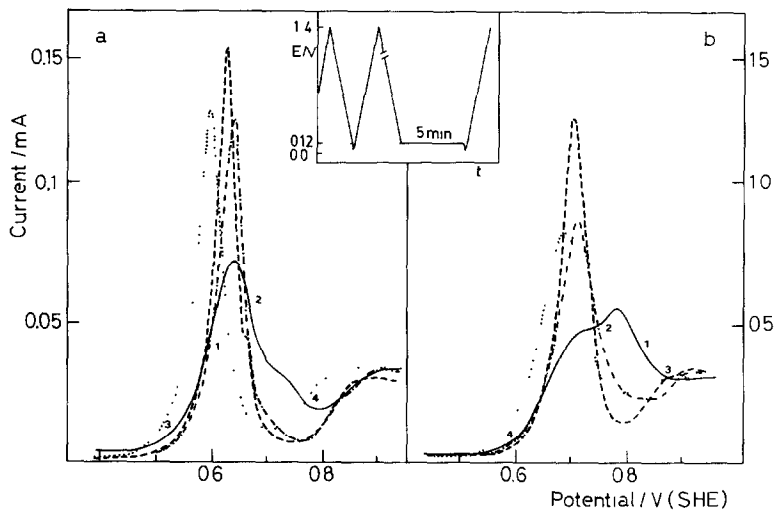

Fig. 1. Voltammograms run at (a) $v = 0.005$ V s^{-1} and (b) $v = 0.05$ V s^{-1}, according to the depicted potential programme, for the different acids. Apparent electrode area: 0.114 cm^2; $R = 70$; 25 °C. (· · · · · ·) 0.05 M $HClO_4$; (— — —) 1 M $HClO_4$; (·–·–·) 0.5 M H_2SO_4; (———) 1 M H_3PO_4. Numbers 1, 2, 3 and 4 indicate reference points used in the calculations as referred to in the text.

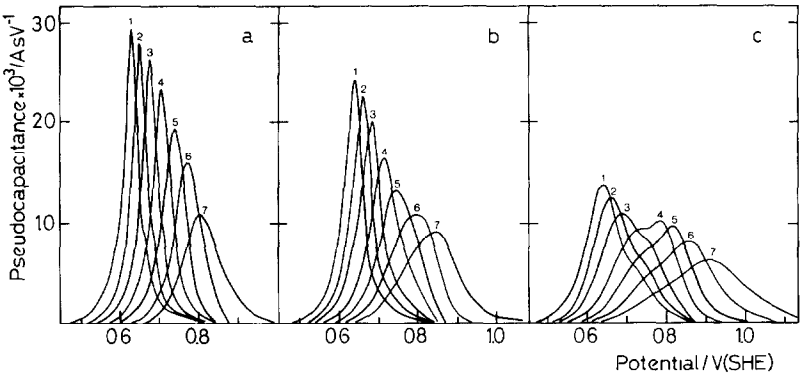

Fig. 2. Pseudocapacitance vs. potential curves for (a) 1 *M* $HClO_4$, (b) 0.5 *M* H_2SO_4 and (c) 1 *M* H_3PO_4. Apparent electrode area: 0.114 cm^2; $R = 70$; 25 °C. Potential programme as depicted in Fig. 1. v/V s^{-1} 0.005 (1); 0.01 (2); 0.02 (3), 0.05 (4); 0.1 (5); 0.2 (6); 0.4 (7).

maxima in the pseudocapacitance–potential plots for 1 *M* H_3PO_4 can be seen clearly. Moreover, as v increases the maximum pseudocapacitances values (C_M) decrease, and ΔE for $C_M/2$, the corresponding halfwidths, increases. At constant v, the values of C_M decrease and those of ΔE for $C_M/2$ increase with the electrolyte composition in the following order: 1 *M* $HClO_4$ > 0.5 *M* H_2SO_4 > 1 *M* H_3PO_4.

The ratios between the total voltammetric oxidation charge (Q_{ox}^T) and the decrease in the H-adatom electrodesorption charge ($\Delta Q_H = Q_H^\circ - Q_H$) due to CO_2 electroadsorption for two different values of R are compared in Table 1. Q_H° is the voltammetric H-adatom electrodesorption charge in the absence of CO_2 adsorbate measured according to the procedure described in the literature [14], and Q_H is that resulting after saturation coverage by the CO_2 adsorbate has been attained. For the three acids, the $Q_{ox}^T/\Delta Q_H$ ratio is always lower than 2, their differences probably being within the limits of the experimental error. For each acid, the ratio is independent of R and exhibits a systematic trend to decrease with v, a fact which appears most notably in H_2SO_4 and H_3PO_4 solutions. These results seem to indicate that the amount of reduced CO_2 adsorbate increases according to the time spent during the negative-going potential scan, in the H-adatom potential range where the CO_2 adsorbate can be anchored to the platinum surface.

Experiments performed in the presence of CO_2 by shifting the lower potential limit stepwise within the H-adatom potential range, show a selective and progressive suppression of the H-adatom electrodesorption current followed by an increase in the oxidation charge related to "reduced" CO_2 adsorbate electrooxidation (Fig. 3). Furthermore, the current peak related to the electrooxidation of the adsorbate produced in the strongly bound H-adatom potential range, is located at potentials more positive than that corresponding to the adsorbate formed in the potential range of weakly bound H-adatoms. This effect can be seen most clearly in 1 *M* H_3PO_4, where two electrooxidation peaks can be distinguished, particularly at the

TABLE 1

Ratio between the total oxidation charge Q_{ox}^{Γ} and the decrease of the H-adatom electrodesorption charge, $\Delta Q_H = Q_H^o - Q_H$ under CO_2 adsorbate saturation conditions, as a function of potential sweep rate in the different electrolytes, for two values of R

v/V s^{-1}	$Q_{ox}^{\Gamma}/\Delta Q_H$			
	0.05 M $HClO_4$	1 M $HClO_4$	0.5 M H_2SO_4	1 M H_3PO_4
$R = 21$				
0.005	1.62 ± 0.15	1.28 ± 0.15	1.43 ± 0.15	1.29 ± 0.15
0.010	1.63	1.27	1.32	1.25
0.020	1.45	1.25	1.23	1 24
0.050	1.36	1.24	1.16	1.21
0.10	1.36	1.20	1.20	1.15
0.20	–	1.29	1.15	1.13
$R = 70$				
0.005	1.46	1.39	1.47	1.31
0.010	1.40	1.19	1.37	1.23
0.020	1.40	1.28	1.33	1.21
0.050	1.37	1.23	1.24	1.19
0.10	–	1.28	1.20	1.16
0.20	–	–	1.14	1.18

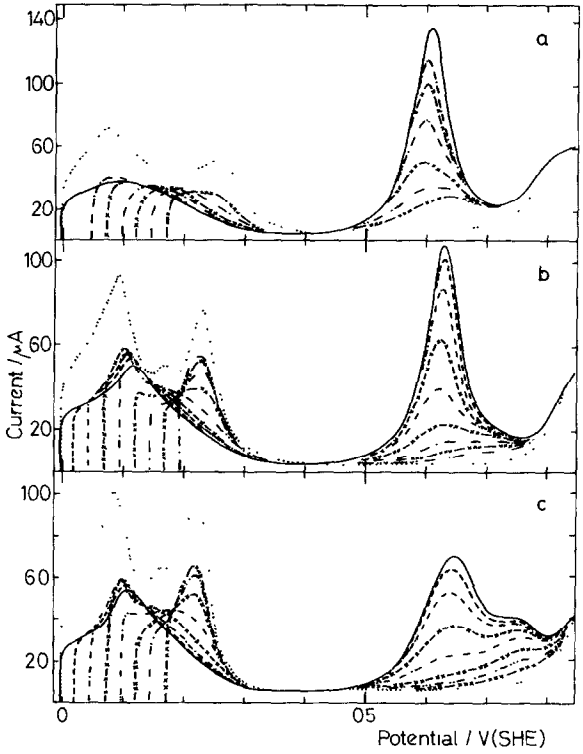

Fig. 3. Dependence of electrooxidation current peak on the lower potential limit. Voltammograms run at 0.010 V s^{-1}. (a) 0.05 M $HClO_4$; (b) 0.5 M H_2SO_4; (c) 1 M H_3PO_4. (· · · · · ·) CO_2-free solutions. Apparent electrode area: 0.114 cm^2; $R = 70$; 25 °C.

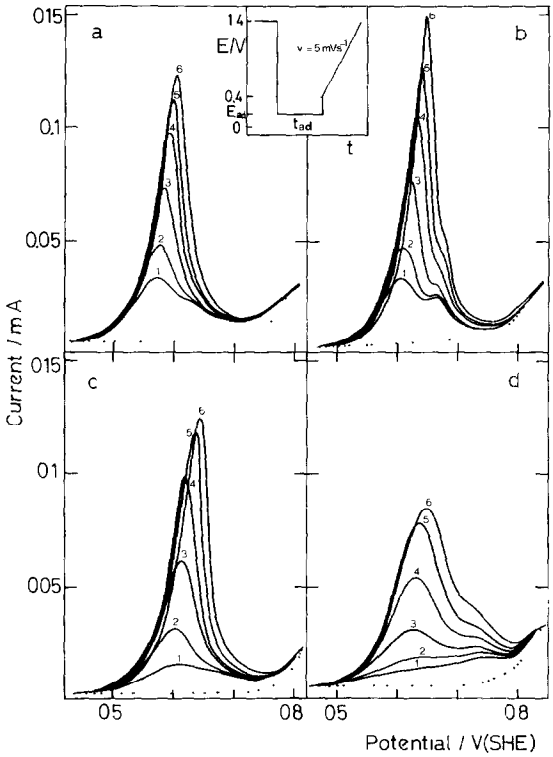

Fig. 4. Dependence of electrooxidation current peak on adsorption time (t_{ad}) at E_{ad}. t_{ad}/s: 10 (1); 15 (2); 30 (3); 60 (4), 120 (5); 300 (6). (a) 0.05 *M* $HClO_4$; (b) 1 *M* $HClO_4$; (c) 0.5 *M* H_2SO_4; (d) 1 *M* H_3PO_4. Apparent electrode area: 0.114 cm^2; $R = 70$; 25 °C. $E_{ad} = 0.07$ V for 0.05 *M* $HClO_4$; $E_{ad} = 0.12$ V for other acids.

highest v values. Moreover, as CO_2 electroadsorption takes place during the negative-going potential sweep, an isopotential region at about 0.175 V can be noticed in the H-adatom electrodesorption profile for both 0.5 *M* H_2SO_4 and 1 *M* H_3PO_4.

The voltammogram for "reduced" CO_2 adsorbate electrooxidation also depends on the adsorption time (t_{ad}) at constant potential (E_{ad}) for the different electrolyte solutions (Fig. 4, see inset potential programme). The value of Q_{ox}^{T} follows a linear dependence on log t_{ad}, with a slope which depends on the solution composition (anion), decreasing in the order 0.05 *M* $HClO_4 > 0.5$ *M* $H_2SO_4 > 1$ *M* H_3PO_4.

Potentiostatic transients

The current transients corresponding to the electrooxidation of "reduced" CO_2 adsorbate run at a constant potential, E_{ox}, depend on E_{ad}, t_{ad} and electrolyte composition (Fig. 5). Thus, in 1 *M* $HClO_4$ the current transient always exhibits three different regions, namely a fast initial decrease, followed by a plateau, and

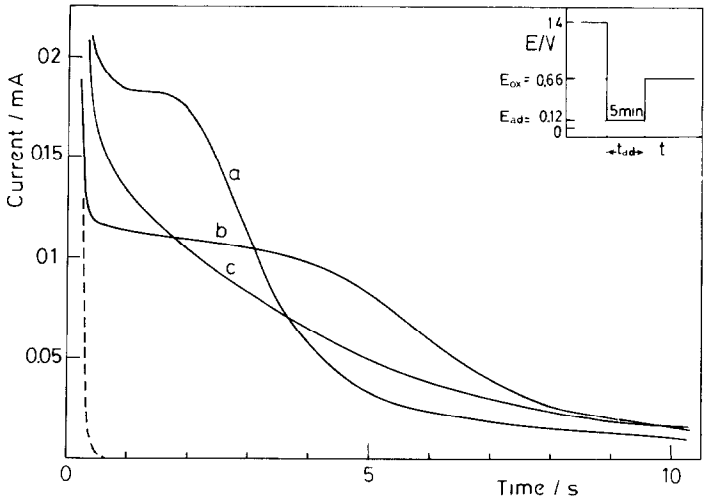

Fig. 5 Potentiostatic current transients for (a) 1 *M* $HClO_4$; (b) 0.5 *M* H_2SO_4; (c) 1 *M* H_3PO_4. (— — —) CO_2-free solutions. $E_{ad} = 0.12$ V; $E_{ox} = 0.66$ V; $t_{ad} = 5$ min. Apparent electrode area: 0.17 cm^2: $R = 21$; 25 °C.

finally a relatively slow decay. The fast initial decrease in current occurs in a range of time which largely exceeds that expected for the double layer charging current effect. The plateau appears when the values of E_{ad} and/or t_{ad} are sufficiently large to saturate the electrode surface with the adsorbate (Fig. 6a, b). Otherwise, intermediate situations between a net current plateau and a continuous current decay can also be observed. For constant E_{ad} and E_{ox}, the location and length of the current plateau depend on t_{ad} (Fig. 6b). Similar conclusions can be drawn from data obtained by changing E_{ox}, and keeping E_{ad} and t_{ad} constant (Fig. 6c). In this case, as one should expect, the electrooxidation reaction becomes faster as E_{ox} moves positively. Under comparable conditions, in 0.05 *M* $HClO_4$, the definition of the current plateau becomes less clear (Fig. 7a, b). The same transient description applies qualitatively to runs made in 0.5 *M* H_2SO_4 (Fig. 8a, b). In this case, however, the best definition of the plateau can be observed.

Current transients run in 1 *M* H_3PO_4 follow the same trend already described for the other electrolyte solutions, although in this case no clear current plateau can be noticed, at least in the range of experimental conditions covered in the present work (Fig. 9a–c).

In general, the shape of the current transient appears to be practically independent of E_{ad} provided that the latter has been set in the weakly bound H-adatom potential range. This is the case particularly for 1 *M* $HClO_4$, where the current transients exhibit clear arrests for $E_{ad} < 0.17$ V (Fig. 6a). Nevertheless, a remarkable difference in the shape and the charge involved in the transients can be noticed when E_{ad} is set within the strongly bound H-adatom potential range. These

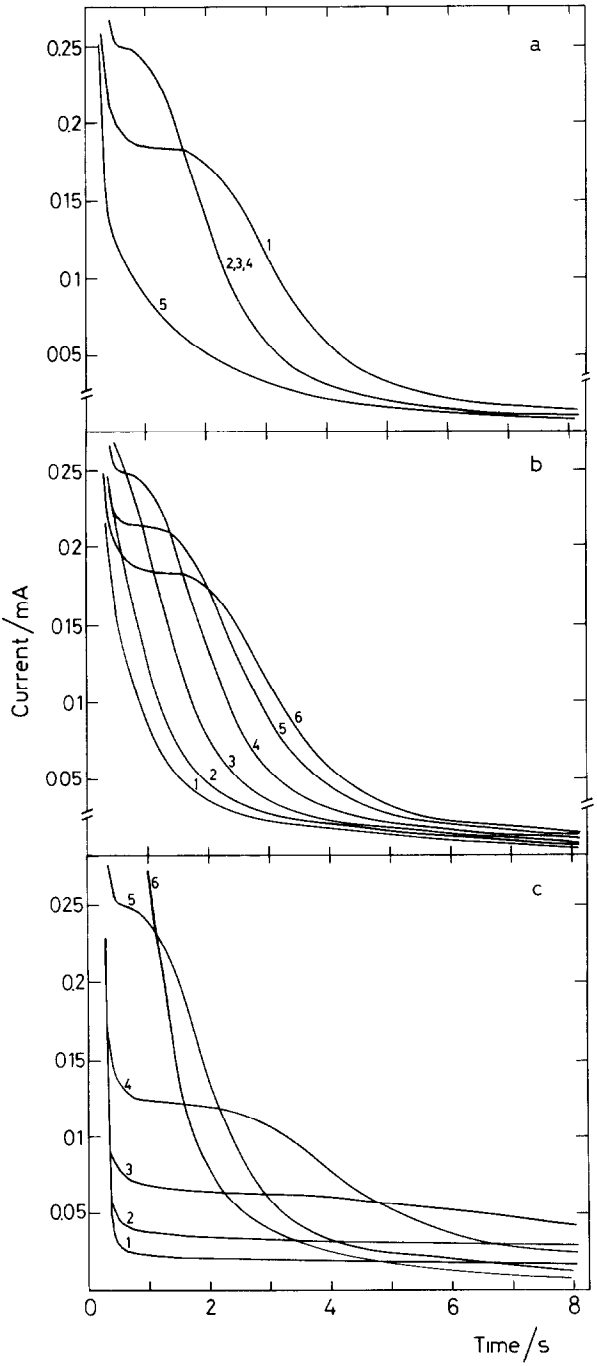

Fig. 6. Potentiostatic current transients in 1 M $HClO_4$ at different E_{ad} and t_{ad}. Apparent electrode area: 0.17 cm^2; $R = 21$; 25 °C. (a) (1) $E_{ad} = 0.12$ V, $t_{ad} = 300$ s; (2) $E_{ad} = 0.07$ V, $t_{ad} = 60$ s; (3) $E_{ad} = 0.12$ V, $t_{ad} = 60$ s; (4) $E_{ad} = 0.17$ V, $t_{ad} = 60$ s; (5) $E_{ad} = 0.22$ V, $t_{ad} = 60$ s. $E_{ox} = 0.66$ V. (b) t_{ad}/s (1) 10; (2) 15; (3) 30; (4) 60; (5) 120; (6) 300. $E_{ad} = 0.12$ V, $E_{ox} = 0.66$ V (c) E_{ox}/V: (1) 0.58; (2) 0.60; (3) 0.62; (4) 0.64; (5) 0.66; (6) 0.68. $E_{ad} = 0.12$ V, $t_{ad} = 60$ s.

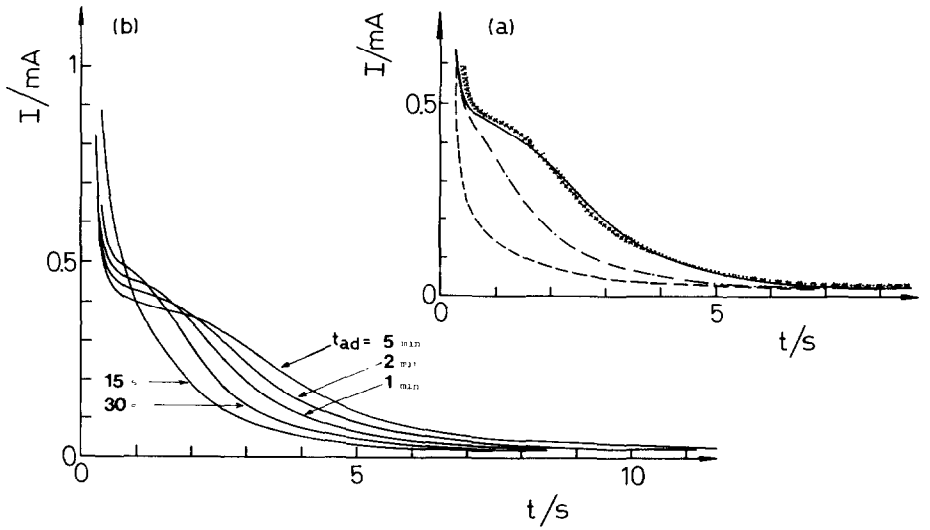

Fig. 7. Potentiostatic current transients in 0.05 M $HClO_4$ at different E_{ad} and t_{ad}. Apparent electrode area: 0.17 cm^2; $R = 21$; 25 °C. (a) E_{ad}/V: 0.0 (× × ×); 0.065 (· · · · · ·); 0.115 (———); 0.165 (· – · – ·); 0.125 (— — —). $E_{ox} = 0.625$ V, $t_{ad} = 60$ s. (b) $E_{ad} = 0.065$ V, $E_{ox} = 0.625$ V and different t_{ad}.

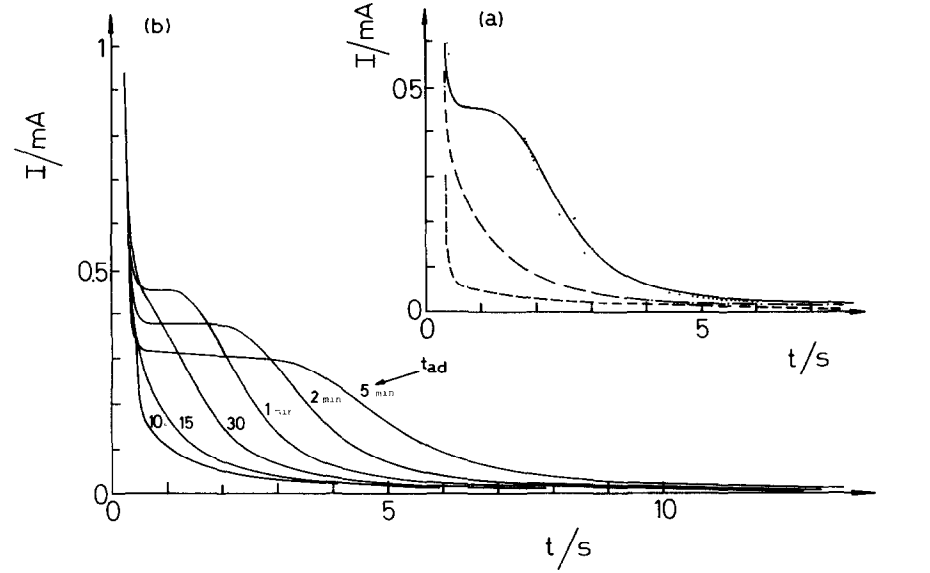

Fig. 8. Potentiostatic current transients in 0.5 M H_2SO_4 at different E_{ad} and t_{ad}. Apparent electrode area: 0.17 cm^2; $R = 21$; 25 °C. (a) E_{ad}/V: 0.065 (· · · · · ·); 0.165 (———); 0.115 (· – · – ·); 0.215 V (— — —). $E_{ox} = 0.665$ V, $t_{ad} = 60$ s. (b) Different t_{ad}. $E_{ad} = 0.115$ V, $E_{ox} = 0.665$ V.

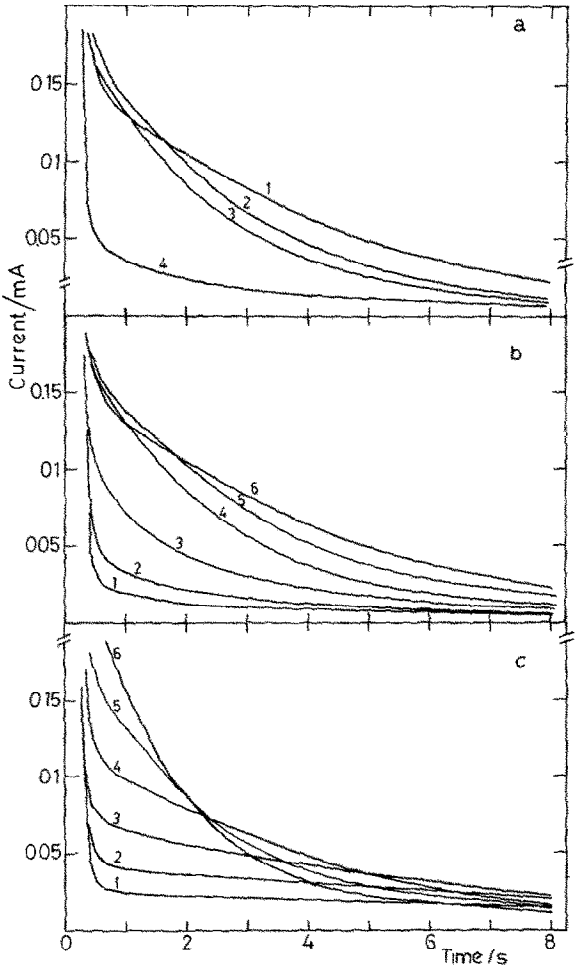

Fig. 9. Potentiostatic current transients in 1 M H_3PO_4 at different E_{ad} and t_{ad}. Apparent surface electrode area: 0.17 cm^2; $R = 21$; 25 °C. (a) (1) $E_{ad} = 0.12$ V, $t_{ad} = 300$ s; (2) $E_{ad} = 0.07$ V, $t_{ad} = 60$ s; (3) $E_{ad} = 0.12$ V, $t_{ad} = 60$ s; (4) $E_{ad} = 0.17$ V, $t_{ad} = 60$ s. $E_{ox} = 0.66$ V. (b) t_{ad}/s: (1) 10; (2) 15; (3) 30; (4) 60; (5) 120; (6) 300. $E_{ad} = 0.12$ V. $E_{ox} = 0.66$ V. (c) E_{ox}/V: (1) 0.58; (2) 0.60; (3) 0.62; (4) 0.64; (5) 0.66; (6) 0.68. $E_{ad} = 0.12$ V, $t_{ad} = 60$ s.

differences, however, tend to disappear as the oxidation charge increases, for instance by increasing t_{ad} (Fig. 6b).

DISCUSSION

Analysis and interpretation of voltammetric data

Both voltammetric and current transient data show that the electrooxidation of "reduced" CO_2 adsorbate formed on electrodispersed platinum in acids is a

complex reaction independent of the roughness factor, but strongly dependent on the electrolyte composition. It is shown that at least two reactions take place, each one within a well-defined potential range. Therefore, for this type of experiment, it is possible to deal, in principle, with each reaction independently, as the overlapping of the corresponding potential windows is relatively small, since two voltammetric peaks can be distinguished.

The analysis of the voltammetric data was based on electrochemical reactions involving adsorbed R- and O-species, so that the general kinetic equation for each voltammetric peak is of the form:

$$j(t)\exp[-\alpha FE(t)/RT] = f(\theta_R\theta_O) \tag{1}$$

where $j(t)$ stands for the instantaneous apparent current density, $E(t)$ denotes the instantaneous applied potential, α is the transfer coefficient assisting the reaction in the anodic direction, and $f(\theta_R, \theta_O)$ is a function of the degree of surface coverage by the "reduced CO_2" adsorbate, θ_R, and the degree of surface coverage by OH species, θ_O, and eventually also involves an interaction energy term. Firstly, $f(\theta_R, \theta_O)$ was tried explicitly as a simple first order function of θ_R, yielding completely unsatisfactory results. Then, a second order dependence of $f(\theta_R, \theta_O)$ on θ_R was assumed. This approach was attempted either directly or by introducing an interaction energy term. Then, for each peak the following expression was used to fit the data:

$$j(t)\exp[-\alpha FE(t)/RT] = k_2\theta_R\theta_O e^{r\theta_R} \tag{2}$$

where k_2 represents a second order rate constant in electrical units and r denotes an interaction parameter.

The application of eqn. (1) to each voltammetric peak requires the knowledge of θ_R and θ_O, which can be evaluated by integration of the function:

$$j(t)\,dE = K\,d\theta \tag{3}$$

where K (A V/cm^2) is a constant which involves the product $k_M v$, where k_M represents the charge density (C/cm^2) for the maximum adsorbate coverage, $\theta_R = 1$, and v (V/s) is the potential sweep rate. The integration of eqn. (3), which gives the values of θ_R and correspondingly of θ_O as a function of E, was performed either from the negative or from the positive potential extreme of the voltammogram. It should be noticed that expressions for $f(\theta_R, \theta_O)$ involving the minimum number of adjustable parameters compatible with curve fitting were used.

For simulating the double peaked voltammograms it was assumed that there are two distinguishable R-species (R_1 and R_2) involved in similar electrochemical reactions, so that the shape of both peaks became the same throughout the different experimental conditions. Then, the two voltammetric components were built up starting from the location of the highest peak in the voltammogram. In this case, the occurrence of different adsorbed R-species makes it useful to add a comment about the kinetic equations involving θ_R and θ_O.

Let us assume that at $t = 0$ the electrode surface is covered by $N_{R1}(0)$ and $N_{R2}(0)$ molecules of species R_1 and R_2, respectively, so that at the initiation of the electrooxidation potential sweep $N_{R1}(0) + N_{R2}(0) = N_T(0)$, where $N_T(0)$ gives the total number of adsorbates of type R at $t = 0$. As the species R1 reacts first, eqn. (2) can be written:

$$j_{2,1}(t) \exp[-\alpha_1 FE(t)/RT] = k'_{2,1} N_{R1}(t) N_0(t) \, e^{r'_1 N_{R1}} \tag{4}$$

where subscripts 2 and 1 stand for the second order reaction involving R1 and $N_{R1}(t)$ and $N_O(t)$ are the instantaneous number of R1 and O species, respectively. As the number of O depends on the number of bare sites produced during the reaction, eqn. (4) results in:

$$j_{2,1}(t) \exp[-\alpha_1 FE(t)/RT] = k_{2,1} N_{R1}(t)[N_{R1}(0) - N_{R1}(t)] \, e^{r_1 N_{R1}(t)} \tag{5}$$

and by defining $\theta_{R1} = N_{R1}(t)/N_{R1}(0)$, this gives

$$j_{2,1}(t) \exp[-\alpha_1 FE(t)/RT] = k_{2,1} \theta_{R1}[1 - \theta_{R1}] \, e^{r_1 \theta_{R1}} \tag{6}$$

Analogously, for the second reaction involving R2, characterized by the rate constant $k_{2,2}$, one can obtain:

$$j_{2,2}(t) \exp[-\alpha_2 FE(t)/RT] = k_{2,2} \theta_{R2}[1 - \theta_{R2}] \, e^{r_2 \theta_{R2}} \tag{7}$$

where $\theta_{R2} = N_{R2}(t)/N_{R2}(0)$. Equations (6) and (7) were employed for the simulation of the voltammograms.

On the other hand, for those voltammograms where the main peak was located at lower potentials (Fig. 1a, full trace), first a calculation of the portion comprised between point 1 and point 2 was made for a single peak. The latter was corrected by subtracting the contribution of the tail extending from the lowest potential up to a region close to point 3. Then, from point 2 to point 4 the calculation was based upon data reconstructed from the portion of the curve starting from point 4. Otherwise, when the main voltammetric peak was located at higher potentials (Fig. 1b, full trace), the calculation of the curve from point 1 to point 2 proceeded on the basis of a single peak corrected for the base current at point 3. Finally, the rest of the voltammogram was calculated by using data reconstructed from the portion of the curve starting at point 4, by considering the base current resulting at the initiation of the voltammetric scan. The selection of the potentials corresponding to points 1 to 4 depended on the conditions of each experiment.

The shape of the voltammogram is determined mainly by the term $f(\theta_R \theta_O)$ in eqn. (1). The best fitting of the voltammetric data was obtained for the set of parameters assembled in Table 2; the simulation of typical voltammograms is depicted in Fig. 10. It should be noted that both $k_{2,1}$ and $k_{2,2}$ increase approximately linearly with v as should be expected for a surface electrochemical reaction under voltammetric conditions. For the same v, the values of $k_{2,1}$ for 0.5 M H_2SO_4 are of comparable magnitude to those of 0.05 M $HClO_4$, but those of 1 M H_3PO_4 are nearly one order of magnitude smaller. In contrast, the values of $k_{2,2}$ are only

TABLE 2

Kinetic parameters resulting from voltammetric data through eqns. (6) and (7). Electrodispersed platinum electrode. $R = 70$

Electrolyte	v/mV s^{-1}	$10^3\, k_{2,1}$/A cm^{-2}	r_1	$10^4\, k_{2,2}$/A cm^{-2}	r_2	$\alpha_1 = \alpha_2$	$k_{2,1}/k_{2,2}$
0.5 *M* H_2SO_4	5	2.1	1.5	1.4	3.3	0.9	15
	10	4.0	1.5	2.3	3.8		18
	20	6.4	1.6	5.5	3.5		12
	50	15	1.5	19	3.0		7.7
	100	23	1.5	48	3.0		4.7
1 *M* H_3PO_4	5	0.32	4.0	1.4	3.0		2.3
	10	0.57	4.0	3.4	3.0		1.7
	20	1.3	3.5	14	2.5		0.95
	50	2.1	4.0	26	3.5		0.80
	100	3.5	3.5	38	4.0		0.90
0.05 *M* $HClO_4$	5	1.8	1.4	2.6	3.0		

slightly dependent on the electrolyte composition. Accordingly, the $k_{2,1}/k_{2,2}$ ratio changes with the solution composition. Finally, the values of r_1 in $HClO_4$ and H_2SO_4 solutions are relatively small as compared to those in H_3PO_4 solution, whereas the values of r_2 are about the same for the three solutions. Finally, the value of $\alpha \simeq 1$ holds for the different electrolyte solutions. The initial deviation of the voltammetric data from the kinetic equation can be taken as an indication that at the early stages of the reaction another process is probably involved, although the latter cannot be analysed separately through voltammetry. On the other hand, the tail of the voltammogram at high positive potentials also exhibits a deviation from the second order rate equation. This deviation should be related to the overlapping of the electrooxidation reaction with the electroformation of the oxide monolayer [15].

Data from the potentiostatic current transients

Further kinetic features of the "reduced CO_2" electrooxidation reaction can be derived from the potentiostatic current transients. The deconvolution procedure applied to the current transients was based on the appearance of three contributions, namely, a first order exponential decay, $j_1(t)$, in the shortest time range, and two second order current decays, $j_{2,1}(t)$ and $j_{2,2}(t)$. When the value of the potential step is set more positive than the potential of the second voltammetric peak, the three reactions should start at $t = 0$. Therefore, $j_T(t)$, the total instantaneous current density, was taken as the sum:

$$j_T(t) = j_1(t) + j_{2,1}(t) + j_{2,2}(t) \tag{8}$$

Let us assume that $j_1(t)$ is due exclusively to a faradaic process, i.e. any double layer charging has been properly corrected. Then the simplest expression for $j_1(t)$ is:

$$j_1(t) = j_{1,0} \exp(-k_1(E_{ox})t) \tag{9}$$

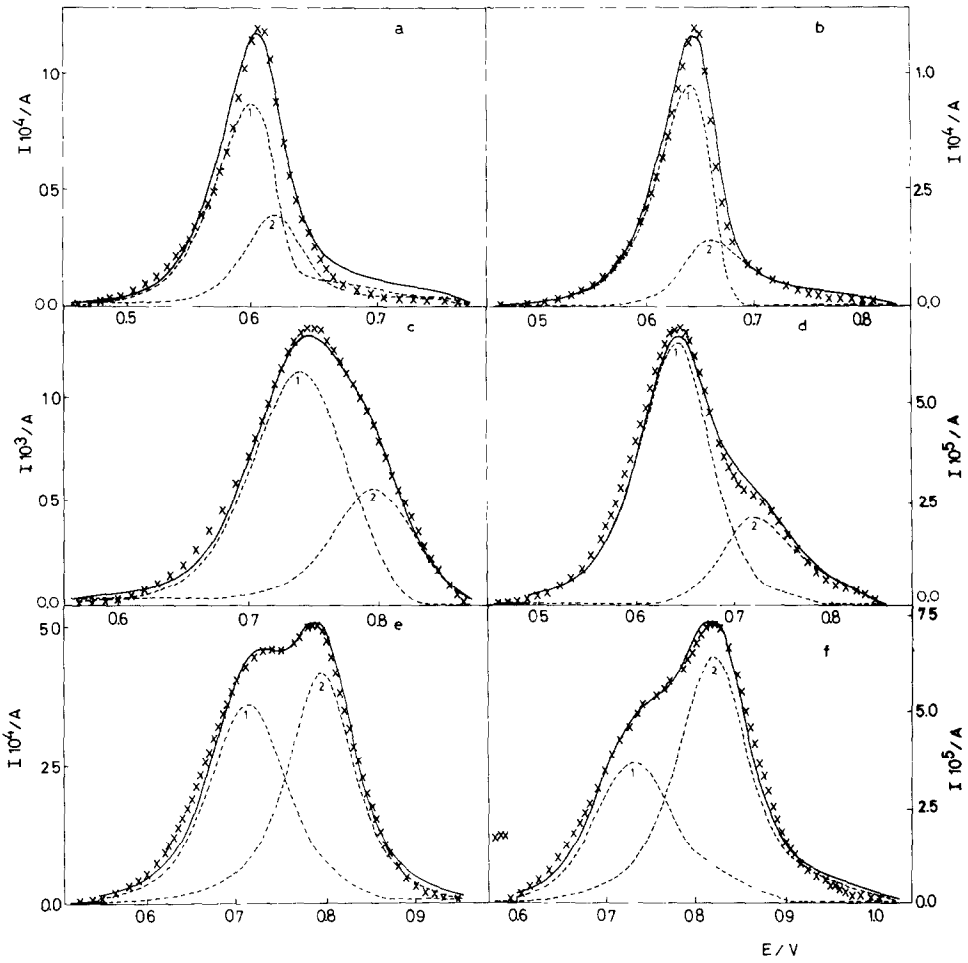

Fig. 10. Simulation of voltammograms. (– – –) Calculated data for contributions 1 and 2; (———) calculated complete voltammogram. (×) Experimental data. (a) $R = 70$; 0.05 M $HClO_4$; $v = 0.005$ V/s; $E_{ad} = 0.065$ V, $t_{ad} = 5$ min. (b) $R = 70$; 0.5 M H_2SO_4; $v = 0.005$ V/s; $E_{ad} = 0.115$ V, $t_{ad} = 5$ min. (c) $R = 70$; 0.5 M H_2SO_4; $v = 0.100$ V/s; $E_{ad} = 0.115$ V, $t_{ad} = 5$ min. (d) $R = 70$; 1 M H_3PO_4; $v = 0.005$ V/s; $E_{ad} = 0.115$ V, $t_{ad} = 5$ min. (e) $R = 70$; 1 M H_3PO_4; $v = 0.050$ V/s; $E_{ad} = 0.115$ V, $t_{ad} = 5$ min. (f) $R = 70$; 1 M H_3PO_4; $v = 0.100$ V/s; $E_{ad} = 0.115$ V, $t_{ad} = 5$ min. Apparent electrode area: 0.114 cm^2.

where $j_{1,0}$ is the value of $j_1(t)$ for $t = 0$ and $k_1(E_{ox})$ is a first order rate constant at the applied potential. For constant potential conditions $k_1(E) = k_1$. First $j_{1,0}$ was estimated from data taken for $t \to 0$. Then, the value of $j_1(t)$ was subtracted from $j_T(t)$ to obtain the sum $j_{2,1}(t) + j_{2,2}(t)$. As the two second order reactions start at $t = 0$, because R1 and R2 are already present at the surface at $t = 0$, and the number of sites for O-species is determined by the degree to which the three reactions take

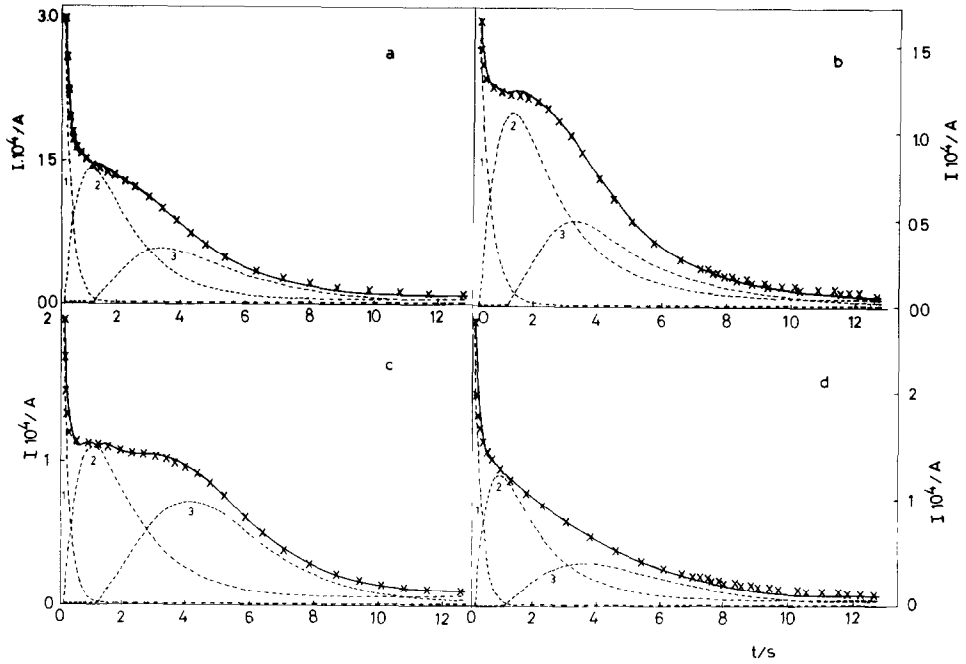

Fig. 11 Simulation of current transients. Dash traces 1, 2 and 3 correspond to data computed for partial reactions and full traces indicate the theoretical current transient. (×) Experimental data. Apparent electrode area: 0.17 cm^2; $R = 21$ (a) 0.05 M $HClO_4$, $E_{ad} = 0.065$ V; $E_{ox} = 0.625$ V; $t_{ad} = 5$ min. (b) 1 M $HClO_4$; $E_{ad} = 0.115$ V, $E_{ox} = 0.645$ V; $t_{ad} = 1$ min. (c) 0.5 M H_2SO_4; $E_{ad} = 0.115$ V; $E_{ox} = 0.665$ V; $t_{ad} = 5$ min. (d) 1 M H_3PO_4; $E_{ad} = 0.115$ V; $E_{ox} = 0.665$ V; $t_{ad} = 5$ min.

place, the resulting expressions for $j_{2,1}(t)$ and $j_{2,2}(t)$ in terms of degrees of surface coverage are:

$$j_{2,1}(t) = k_{2,1}(E_{ox})\theta_{R1}(t)\left[1 - \theta_{R1}(t) - \theta_{R2}(t) - \theta_1(0)\, e^{k_1 t}\right] e^{r_1\theta_{R1}(t)} \tag{10}$$

and

$$j_{2,2}(t) = k_{2,2}(E_{ox})\theta_{R2}(t)\left[1 - \theta_{R1}(t) - \theta_{R2}(t) - \theta_1(0)\, e^{k_1 t}\right] e^{r_2\theta_{R2}(t)} \tag{11}$$

where $\theta_{R1}(0) + \theta_{R2}(0) + \theta_1(0) = 1$ at $t = 0$, and $k_{2,1}(E_{ox})$ and $k_{2,2}(E_{ox})$ are the rate constants in electrical units at the potential E_{ox}. Equations (10) and (11) yield $j_{2,1}(t) = j_{2,2}(t) = 0$ for both $t = 0$ and for $t \to \infty$. The exponential factors containing r_1 and r_2, respectively, represent interaction terms, which depend on the degree of surface coverage and are characterized by r_1 and r_2.

A comparison of the experimental current transients with those resulting from the deconvolution procedure is given in Fig. 11. The corresponding adjustable parameters are assembled in Table 3. It should be noted further that the values of $\theta_1(0)$, $\theta_{R1}(0)$ and $\theta_{R2}(0)$ depend on the electrolyte composition.

The largest difference in the values of $k_{2,1}$ and $k_{2,2}$ of the second order reactions is about 20 for 0.5 M H_2SO_4. The values of $k_{2,1}$ and $k_{2,2}$ as well as the values of r_1

TABLE 3

Data resulting from the analysis of potentiostatic transients in different electrolytes. Electrodispersed Pt. $R = 21$; $T = 25\,^{\circ}C$

Solution	E_{ad}/V(RHE)	t_{ad}/min	E_{ox}/V(RHE)	k_1/s^{-1}	$\theta_1(0)$	$10^3\, k_{2,1}$/A cm^{-2}	$\theta_{R1}(0)$	$10^3\, k_{2,2}$/A cm^{-2}	$\theta_{R2}(0)$	r_{R1}	r_{R2}
0.05 *M* $HClO_4$	0.065	5	0.625	4.6	0.10	2.1	0.65	2.2	0.25	2.2	1.3
1 *M* $HClO_4$	0.115	1	0.645	2.9	0.10	2.0	0.55	1.2	0.35	2.8	2.2
0 5 *M* H_2SO_4	0.115	5	0.665	5.1	0.06	3.3	0.45	1.9	0.49	3.5	0.4
1 *M* H_3PO_4	0.115	5	0.665	4.9	0.10	2.0	0.60	1.6	0.30	2.6	0.3

and r_2, $\theta_{R1}(0)$ and $\theta_{R2}(0)$ are comparable to those found under voltammetric conditions. The difference in the kinetic data assembled in Tables 2 and 3 can be attributed firstly to the fact that in voltammetric calculations the first order reaction was ignored, and secondly to the specific potential control conditions, either voltammetric or potentiostatic, respectively.

Mechanistic interpretation

The kinetic analysis of reduced CO_2 electrooxidation indicates the participation of at least three distinguishable processes. The first order reaction at short times appears to be practically independent of the solution composition, whereas the two second order processes show a difference depending on whether they take place in $HClO_4$, H_2SO_4 or H_3PO_4 solution. The relative contribution of each process to the entire reaction at a fixed time depends on the history of the electrooxidation process itself.

The first order electrooxidation reaction starting from the most compact electroadsorbate structure plays an important role as it begins to produce free sites for OH electroadsorption. Hence, for $\theta_T \to 1$, following the probable reduced CO_2 adsorbate stoichiometry discussed previously [13] the reaction can be written as follows:

$$[Pt_3(H_3CO_2)_{ad}(H_2O)Pt] \to CO_2 + 3\,H^+ + H_2O + 4\,Pt + 3\,e^- \tag{12}$$

The second order equations can be justified with the usual formalism of electrochemical kinetics in terms of either adsorbates with different stoichiometries or of a common adsorbate located on different adsorption sites. As to latter, it is well known that the pc Pt surface involves at least two main types of adsorption sites, namely those for strongly bound and loosely bound H atoms. These concepts can be extended to reduced CO_2 adsorbates, since it has been shown previously that CO_2 electroadsorption occurs selectively. Firstly, CO_2 reacts with strongly adsorbed H atoms, and subsequently it does so with loosely bound H adatoms [13]. This means that at least two energetically different reduced CO_2 adsorbates can be produced. These adsorbates can be assigned to the R1- and R2-species, respectively. Hence, in the presence of adsorbed OH ($\theta_O = \theta_{OH}$), the overall electrooxidation reactions involving R1- and R2-species appear to be determined kinetically by a similar type of second order electrochemical reaction involving the reduced CO_2 electroadsorbate and adsorbed OH produced throughout the preceding water discharge reaction on bare Pt sites. This can be expressed through the following formal reactions:

$$Pt + H_2O \rightleftharpoons Pt(OH)_{ad} + H^+ + e^- \tag{13}$$

$$Pt[HCO_2]_{R1} + (OH)_{ad} \Rightarrow CO_2 + H_2O + H^+ + Pt + e^- \tag{14}$$

$$Pt[HCO_2]_{R2} + (OH)_{ad} \to CO_2 + H_2O + H^+ + Pt + e^- \tag{15}$$

For simplicity, the adsorbates R_1 and R_2 represented as $Pt[HCO_2]_{R1}$ and $Pt[HCO_2]_{R2}$, respectively, without commitment to any particular stoichiometry for

each electroadsorbate. Probably the former adsorbate corresponds to the most reduced species, approaching $[Pt_3(H_3CO_2)]_{ad}$, whereas the latter can be assigned to the least reduced species, such as $[Pt(HCO_2)]_{ad}$, although the determination of the corresponding stoichiometries is beyond the possibilities of the present work.

Let us assume that the two second order electrochemical processes involving R1- and R2-species approach quasi-equilibrium conditions for a limited time window and that OH, R1- and R2-adsorbates interact with each other. Then, for reaction (14) one obtains:

$$j_{2,1} = k^{\circ}_{2,1}\theta_{R1}\theta_{OH} \exp\left[(1-\gamma_{R1})\frac{g_{R1}\theta_T}{RT}\right] \exp\left[(1-\theta_{OH})\frac{g_{OH}\theta_T}{RT}\right] \exp\left[\frac{EF}{RT}\right] \tag{16}$$

and provided that $\theta_{OH} = 1 - \theta_{R1}$, eqn (16) becomes:

$$j_{2,1} = k^{\circ}_{2,1}\theta_{R1}(1-\theta_{R1}) \exp\left[-\frac{\theta_T}{RT}\left[(1-\gamma_{R1})g_{R1} + (1-\gamma_{OH})g_{OH}\right]\right] \exp\left[\frac{EF}{RT}\right] \tag{17}$$

Analogously, for reaction (15) the rate equation is:

$$j_{2,2} = k^{\circ}_{2,2}\theta_{R2}(1-\theta_{R1}-\theta_{R2}) \exp\left[-\frac{\theta_T}{RT}\left[(1-\gamma_{R2})g_{R2} + (1-\gamma_{OH})g_{OH}\right]\right] \exp\left[\frac{EF}{RT}\right] \tag{18}$$

where $k^{\circ}_{2,1}$ and $k^{\circ}_{2,2}$ are the rate constants in electrical units at the reference potential of each reaction, γ_{R1} and γ_{R2} are the corresponding symmetry coefficients, and g_{R1} and g_{R2} the corresponding interaction coefficients in energy units. From eqns. (16) and (17):

$$r_{R1} = -\left[(1-\gamma_{R1})g_{R1} + (1-\gamma_{OH})g_{OH}\right]/RT \tag{19}$$

and

$$r_{R2} = -\left[(1-\gamma_{R2})g_{R2} + (1-\gamma_{OH})g_{OH}\right]/RT \tag{20}$$

Therefore, the rate equations (17) and (18) are of the form:

$$j \simeq \theta_R(1-\theta_R) \exp(r_R\theta_T) \exp[FE/RT] \tag{21}$$

involving a value of $\alpha = 1$. This is precisely the type of basic second order rate equation used in the deconvolution of the voltammograms and current transients.

In terms of adsorption isotherms, eqns. (17) and (19) are consistent with a Temkin-type adsorption isotherm, implying considerable adsorbate–adsorbate interaction effects. However, no further conclusions can be derived from the interaction parameters at present due to the complexity of the electrochemical reaction.

The occurrence of reactions (12)–(15) during the global electrooxidation reaction can explain the intermediate eps (electron per Pt site) values lying between 1 and 2, reported in Table 1, over the entire change in the relative contribution of each process in the entire reaction. Those three reactions also account for the departure of the initial and final parts of the voltammograms from the expectation of single second order surface processes valid in the entire potential range where the complete "reduced CO_2" electrooxidation takes place.

The fact that the ratio $k_{2,1}/k_{2,2}$ depends on v (Table 2) can be explained in terms of the same reaction scheme if a conversion of species R2 into species R1 occurs at the surface level. This type of process has already been described in previous work on the electrooxidation of adsorbed CO on platinum. In that case R2 and R1 referred to bridge and linear bonded CO-adsorbates on polycrystalline platinum [15].

Reactions (14) and (15) probably imply different structures for the "reduced" CO_2 adsorbates, which besides being sensitive to the crystalline faces of platinum, should depend also on the applied potential. In this respect, there is evidence that the structures of adsorbates formed on well-defined platinum surfaces, such as those resulting from CO adsorption and other comparable adsorbates obtained from organic fuels, depend on E_{ad}, on θ_T, and on the electrooxidation potential programme [15–19]. As discussed previously [13,20], the structure of the "reduced" CO_2 adsorbate can be considered as an ensemble consisting of Pt sites, H-adatoms, H_2O and CO_2 molecules, where the ratio of the components involved in the ensemble unit changes according to the potential [6,7,19]. This assumption is consistent with the most recent work on the structure of water at the electrical double layer and its dependence on the solution composition and applied potential [21–23]. In the case of "reduced" CO_2 adsorbate, as discussed previously [13] the initial stoichiometry resulting at $E_{ad} = 0.12$ V is consistent with a platinum surface coverage of H-adatoms of ca. 25% under electroadsorbate saturation.

The influence of the electrolyte composition on the electrooxidation reaction can be explained through the interaction of anions with adsorbed OH-species and water resulting mainly from H-bonding. For the second order processes, the decrease in the values of $k_{2,1}$ and $k_{2,2}$ in going from $HClO_4$ and H_2SO_4 acid solutions to H_3PO_4 acid solutions is correlated with the corresponding increase in the anion–water interaction energy through H-bonding [16,24]. In this case, the voltammograms show that the splitting of the electrooxidation peak becomes enhanced considerably in going from $HClO_4$ to H_2SO_4 and to H_3PO_4 solutions. The strength of the acids correlates with the fact that the probability of H-bonding increases in the order $H_2PO_4^- > HSO_4^- \simeq ClO_4^-$ [19,24]. This influence of the strength of the acids has also been observed qualitatively for other reactions such as H-adatom electroadsorption–electrodesorption, and the more complicated electrooxidation of glucose residues on platinum in acids [25].

CONCLUSIONS

The kinetics of the electrooxidation of "reduced" CO_2 electroadsorbate on electrodispersed platinum can be interpreted as three distinguishable processes. The distinction of each reaction becomes feasible through the use of electrodispersed platinum electrodes involving a defined and reproducible topography where the influence of impurities on the surface reaction is minimized. The initial first order process explains the triggering of the electrooxidation reaction because it creates sites for OH-adsorption from water electrooxidation. This reaction appears to be

rather insensitive to changes in the solution composition. One can also distinguish two second order surface electrochemical processes comprising at least two "reduced CO_2" adsorbates and OH-adsorbed species. The adsorbates imply anion–H_2O–CO_2–H-bonding interactions which depend to a large extent on the solution composition. The present analysis of the results allows us to establish quantitative data related to the kinetics of the different processes and to explain the values for the numbers of electrons per site ranging between 1 and 2 for the overall reaction.

ACKNOWLEDGEMENTS

This work was supported financially by the Dirección General de Investigación Científica y Técnica (PB-86-0565), the Regional Program for the Scientific and Technological Development of the Organization of American States. A.J.A. and M.C.G. thank the Universidad Nacional de La Plata for leave of absence.

REFERENCES

1 J. Giner, Electrochim. Acta, 8 (1963) 867; 9 (1964) 63.
2 M.W. Breiter, Electrochim. Acta, 12 (1967) 1213; J. Electroanal. Chem., 19 (1968) 131.
3 S.B. Brummer and K. Cahill, J. Electroanal. Chem., 21 (1969) 463.
4 J. Sobkowski and A. Czerwinski, J. Electroanal. Chem., 55 (1974) 391; ibid., 65 (1975) 327.
5 A. Czerwinski and J. Sobkowski, J. Electroanal. Chem., 59 (1975) 41.
6 V.N. Andreev, Yu. B. Vasil'ev, N.V. Osetrova and T.N. Yastrebova, Elektrokhimiya, 19 (1983) 381.
7 A.A. Mikhailova, N.V. Osetrova and Yu.B. Vasil'ev, Elektrokhimiya, 21 (1985) 1051.
8 N.A. Maiorova, A.A. Mikhailova, O.A. Khazova and Yu.B Vasil'ev, Elektrokhimiya, 22 (1986) 96.
9 E.P. Leiva and M.C. Giordano, J. Electroanal. Chem., 189 (1985) 257.
10 E.P. Leiva, A.M. Baruzzi and M.C. Giordano, J. Electroanal. Chem., 158 (1983) 103
11 A.C. Chialvo, W.E. Triaca and A.J. Arvia, J. Electroanal. Chem., 146 (1983) 93.
12 L. Vásquez, J. Gómez, A.M. Baró, N. García, M.L. Marcos, J. González-Velasco, J.M. Vara, A.J. Arvia, J. Presa, A. García and M. Aguilar, J. Am. Chem. Soc., 109 (1987) 1730.
13 M.L. Marcos, J.M. Vara Cuadrado, J. González-Velasco and A.J. Arvia, J. Electroanal. Chem., 224 (1987) 189.
14 D.A.J. Rand and R. Wood, J. Electroanal. Chem., 35 (1972) 209.
15 S.A. Bilmes, N.R. de Tacconi and A.J. Arvia, J. Electroanal. Chem., 164 (1984) 129; 177 (1984) 201.
16 S.A. Bilmes, M.C. Giordano and A.J. Arvia, J. Electroanal. Chem., 225 (1987) 183; Can. J. Chem., 66 (1988) 2259.
17 B. Beden, F. Hahn, S. Juanto, C. Lamy and J.-M. Léger, J. Electroanal. Chem., 225 (1987) 215; 237 (1987) 119.
18 B. Beden, F. Hahn, C. Lamy, J.-M. Léger, N.R. de Tacconi, R.O. Lezna and A.J. Arvia, in preparation.
19 A.M. Castro Luna, M.C. Giordano and A.J. Arvia, J. Electroanal. Chem., 259 (1989) 173.
20 V.E. Kazarinov, V.N. Andreev and G.Ya. Tysyachnaya, Elektrokhimiya, 8 (1972) 927.
21 A. Bewick, K. Kunimatsu, J. Robinson and J.W. Russell, J. Electroanal. Chem., 119 (1981) 175.
22 A. Bewick and J. Russell, J. Electroanal. Chem., 132 (1982) 329.
23 F.T. Wagner and T.E. Moylan, Surf. Sci., in press.
24 C.I. Ratcliffe and J.A. Ripmeester, J. Phys. Chem., 90 (1986) 1259.
25 M.F.L. de Mele, R.C. Salvarezza, V.D. Vásquez Moll, H.A. Videla and A.J. Arvia, J. Electrochem. Soc., 133 (1986) 746.